DOI: 10.1002/ejic.200500438

Synthesis and Characterization of Dinuclear Europium Complexes Showing Pure Red Electroluminescence

Hyosook Jang,[a] Chang-Hwan Shin,[a] Byung-Jun Jung,[b] Do-hyeon Kim,[a] Hong-Ku Shim,*[b] and Youngkyu Do*[a]

Keywords: Electroluminescence / Europium / Dinuclear complexes / 2,2′-Bipyrimidine

Two dinuclear Eu^{III} complexes have been synthesized by employing β-diketones and 2,2′-bipyrimidine (bpm) as sensitizing ligands for the Eu ion and a bridging ligand, respectively, and characterized by various means including single-crystal X-ray crystallography. The use of dibenzoylmethane (dbm) and trifluorothenoylacetone (tta) as β-diketones gave $[Eu_2(dbm)_6(bpm)]$ (**1**) and $[Eu_2(tta)_6(bpm)]$ (**2**). Both show strong intermolecular π–π interactions that may be responsible for their high melting points. The analysis of the absorption, excitation, and emission spectra of the dinuclear complexes along with a comparison with analogous mononuclear complexes containing the same β-diketone ligands and 1,10-phenanthroline (phen) suggests that the dinuclear complexes follow the luminescence mechanism of general Ln^{III} complexes. An EL device with the structure ITO/PEDOT/PVK + PBD + **1** 10 wt.-%/LiF/Al shows pure red emission with an efficiency similar to those of mononuclear complexes.

Introduction

Luminescent metal complexes are attractive due to their potential applications in the development of organic light-emitting diodes (OLEDs),[1] sensors,[2] and molecular optoelectronic devices.[3] In particular, various metal complexes for OLEDs have been intensively studied and developed;[4,5] typical examples are lanthanide complexes.[5] Electroluminescent (EL) lanthanide complexes have the advantages of extremely narrow emission spectra and the possibility of high EL efficiency caused by the intramolecular energy transfer that consists of the absorption of energy by organic ligands, intersystem crossing into a triplet state of the organic ligands, and energy transfer to the central lanthanide cation.[5] Among lanthanide complexes, Eu^{III} complexes are of particular interested because of their red emission. However, europium systems still require improvement in color purity, carrier-transporting, and thermal stability for practical use.

Although a number of mononuclear lanthanide complexes have been used in OLEDs,[5] examples of electroluminescent dinuclear lanthanide systems are very rare and to date $[Tb_2(acac\text{-}azain)_4(\mu\text{-}acac\text{-}azain)_2]$ [acac-azain = 1-(*N*-7-azaindolyl)-1,3-butanedionato], a green emitter in electroluminescent devices, is the only reported system.[6] Other dinuclear lanthanide complexes based on pyridylamine ligands (Eu^{III}, Tb^{III}, and Dy^{III}),[7] diketonate ligands (Eu^{III}, Nd^{III}, and Sm^{III}),[8] calix[8]arene (Eu^{III}),[9] and N,N,O donor ligands (Sm^{III}, Eu^{III}, Tb^{III}, and Dy^{III};[10a] La^{III}–Lu^{III}[10b]) are known to display photoluminescence. It should also be noted that the lanthanide complexes $[Eu_xTb_{1-x}(acac)_3(phen)]$ (x = 0–1)[11] employed in white-

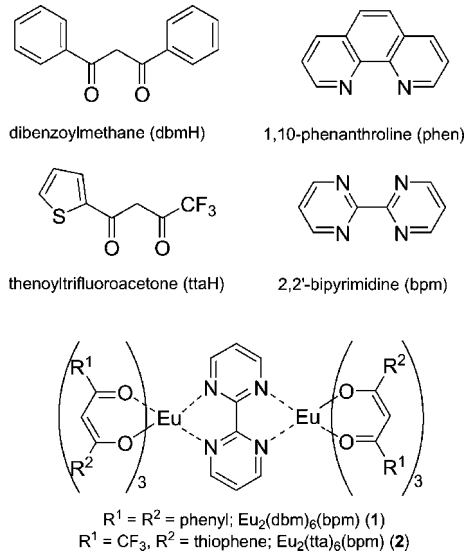

Figure 1. Molecular structures and abbreviations of the materials.

[a] Department of Chemistry, School of Molecular Science-BK21 and Center for Molecular Design and Synthesis, Korea Advanced Institute of Science and Technology,
Daejeon, 305-701, Republic of Korea
Fax: +82-42-869-2810
E-mail: ykdo@kaist.ac.kr
[b] Department of Chemistry, School of Molecular Science-BK21 and Center for Advanced Functional Polymers, Korea Advanced Institute of Science and Technology,
Daejeon, 305-701, Republic of Korea
E-mail: hkshim@kaist.ac.kr

Supporting information for this article is available on the WWW under http://www.eurjic.org or from the author.

light-emitting OLEDs have been claimed to be dinuclear systems, although in the absence of characterization data it is difficult to consider them as legitimate dinuclear systems. To lessen the scarcity of electroluminescent dinuclear lanthanide system, we have designed and synthesized a set of dinuclear Eu^{III} complexes based on 2,2′-bipyrimidine (bpm) as a bridging ligand and β-diketones (L) as sensitizing ligands (Figure 1). We reported here the details of the synthesis, structures, and luminescence characteristics of $[Eu_2L_6(bpm)]$ [L = dibenzoylmethane (dbm) **1** and thenoyltrifluoroacetone (tta) **2**].

Results and Discussion

Syntheses and Structures

The dinuclear Eu^{III} complexes $[Eu_2L_6(bpm)]$ (L = dbm, tta) were prepared in moderate yields by the reaction of $EuCl_3·6H_2O$, the corresponding β-diketone ligand, and bpm in a 2:6:1 molar ratio and fully characterized by various means. The use of $EuCl_3·6H_2O$, β-diketone ligand, and bpm in 1:3:1 molar ratio, a stoichiometric ratio for the as-yet-unknown mononuclear complex $[EuL_3(bpm)]$, also resulted in the formation of the corresponding dinuclear species. It is interesting to note that this reaction chemistry of Eu^{III} was not similarly applied to diamagnetic La^{III} since the analogous reaction systems with $LaCl_3·7H_2O$ gave mononuclear $[LaL_3(bpm)]$, as judged by ^1H NMR spectroscopy. The unavailability of mononuclear $[EuL_3(bpm)]$ led us to select the known complexes $[EuL_3(phen)]$[12] (L = dbm **3** and tta **4**) as closely corresponding mononuclear systems for comparison purposes. (Figure 1) The dinuclear Eu^{III} complexes were initially isolated as solvates $[Eu_2L_6(bpm)]·2(solvent)$ (solvent = Et_2O for **1** and THF for **2**) but the desolvated forms, confirmed by TGA and elemental analysis, were used for measurement purpose except the single-crystal X-ray diffraction studies. They are soluble in common organic solvents and **1** shows better solubility than **2**. Their solubility is similar to that of the corresponding mononuclear complexes **3** and **4**. They are air-stable both in the solid state and in solution. The thermal stability of the dinuclear systems, estimated by the temperature T_{d5} causing 5% weight loss, is also similar to that of the corresponding mononuclear compounds, although the dinuclear species tend to have higher melting points than the mononuclear complexes.

The molecular structures of **1**·$2Et_2O$ and **2**·2THF are depicted in Figures 2 and 3, respectively. Selected bond lengths and angles are summarized in Tables 1 and 2. Compound **1** has two eight-coordinate Eu^{III} sites that are separated by 7.011 Å and symmetrically related by an inversion center lying on the planar bpm moiety. The coordination sphere of each Eu center in **1** can be best described as a distorted square antiprism (Figure 4, a). The average Eu–O bond length is 2.343 Å and the average Eu–N bond length

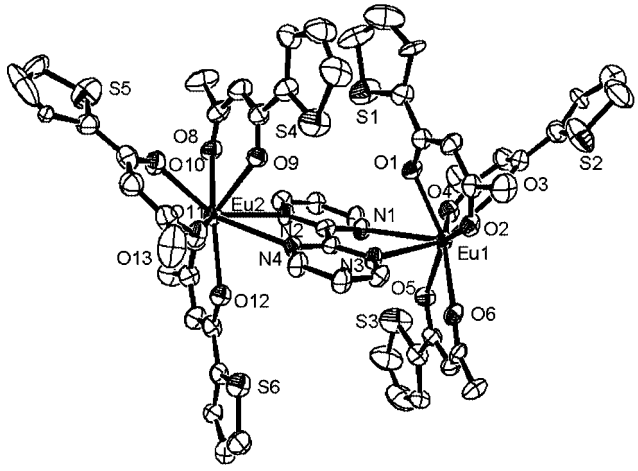

Figure 3. Molecular structure of **2**·2THF. Thermal ellipsoids are drawn at the 30% probability level. The hydrogen and fluorine atoms and tetrahydrofuran molecules have been omitted for clarity.

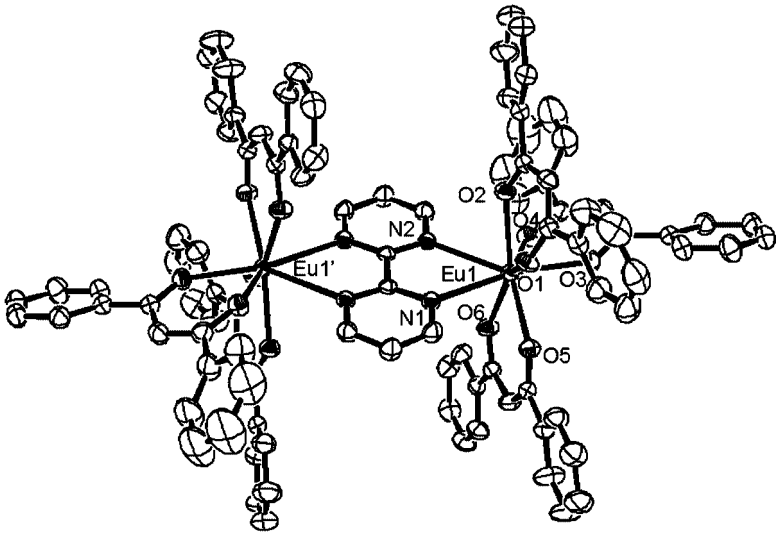

Figure 2. Molecular structure of **1**·$2Et_2O$. Thermal ellipsoids are drawn at the 30% probability level. The hydrogen atoms and diethyl ether molecules have been omitted for clarity.

Table 2. Selected bond lengths [Å] and angles [°] for **2**·2THF.

Eu(1)–O(1)	2.404(7)	Eu(1)–O(2)	2.382(7)	Eu(1)–O(3)	2.447(8)
Eu(1)–O(4)	2.373(8)	Eu(1)–O(5)	2.381(7)	Eu(1)–O(6)	2.433(8)
Eu(1)–O(7)	2.525(8)	Eu(1)–N(1)	2.699(8)	Eu(1)–N(3)	2.679(9)
Eu(2)–O(8)	2.399(8)	Eu(2)–O(9)	2.370(8)	Eu(2)–O(10)	2.392(8)
Eu(2)–O(11)	2.354(8)	Eu(2)–O(12)	2.382(8)	Eu(2)–O(13)	2.406(8)
Eu(2)–O(14)	2.612(9)	Eu(2)–N(2)	2.664(9)	Eu(2)–N(4)	2.703(8)
O(1)–Eu(1)–O(2)	73.0(2)	O(1)–Eu(1)–O(3)	72.6(3)	O(1)–Eu(1)–O(4)	86.4(3)
O(1)–Eu(1)–O(5)	135.6(2)	O(1)–Eu(1)–O(6)	135.1(3)	O(1)–Eu(1)–O(7)	140.6(3)
O(2)–Eu(1)–O(3)	70.6(3)	O(2)–Eu(1)–O(4)	139.3(3)	O(2)–Eu(1)–O(5)	144.5(3)
O(2)–Eu(1)–O(6)	73.8(3)	O(2)–Eu(1)–O(7)	92.1(3)	O(3)–Eu(1)–O(4)	69.9(3)
O(3)–Eu(1)–O(5)	130.5(3)	O(3)–Eu(1)–O(6)	122.2(3)	O(3)–Eu(1)–O(7)	68.0(3)
O(4)–Eu(1)–O(5)	72.8(3)	O(4)–Eu(1)–O(6)	137.9(3)	O(4)–Eu(1)–O(7)	81.9(3)
O(5)–Eu(1)–O(6)	70.7(2)	O(5)–Eu(1)–O(7)	75.6(3)	O(6)–Eu(1)–O(7)	69.4(3)
O(1)–Eu(1)–O(1)	66.8(3)	N(1)–Eu(1)–O(2)	125.4(3)	N(1)–Eu(1)–O(3)	125.9(3)
N(1)–Eu(1)–O(4)	73.3(3)	N(1)–Eu(1)–O(5)	69.8(3)	N(1)–Eu(1)–O(6)	111.8(3)
N(1)–Eu(1)–O(7)	142.0(3)	N(3)–Eu(1)–O(1)	72.4(3)	N(3)–Eu(1)–O(2)	73.5(3)
N(3)–Eu(1)–O(3)	135.5(3)	N(3)–Eu(1)–O(4)	133.4(3)	N(3)–Eu(1)–O(5)	93.9(3)
N(3)–Eu(1)–O(6)	69.8(3)	N(3)–Eu(1)–O(7)	139.1(3)	N(1)–Eu(1)–N(3)	60.2(3)
O(8)–Eu(2)–O(9)	71.9(3)	O(8)–Eu(2)–O(10)	69.9(3)	O(8)–Eu(2)–O(11)	136.7(3)
O(8)–Eu(2)–O(12)	143.0(3)	O(8)–Eu(2)–O(13)	73.6(3)	O(8)–Eu(2)–O(14)	107.7(3)
O(9)–Eu(2)–O(10)	77.4(3)	O(9)–Eu(2)–O(11)	80.5(3)	O(9)–Eu(2)–O(12)	131.9(2)
O(9)–Eu(2)–O(13)	139.4(3)	O(9)–Eu(2)–O(14)	141.7(3)	O(10)–Eu(2)–O(11)	71.9(3)
O(10)–Eu(2)–O(12)	134.9(3)	O(10)–Eu(2)–O(13)	109.7(3)	O(10)–Eu(2)–O(14)	67.3(3)
O(11)–Eu(2)–O(12)	79.9(3)	O(11)–Eu(2)–O(13)	140.0(3)	O(11)–Eu(2)–O(14)	74.9(3)
O(12)–Eu(2)–O(13)	71.8(3)	O(12)–Eu(2)–O(14)	71.9(3)	O(13)–Eu(2)–O(14)	69.9(3)
N(2)–Eu(2)–O(8)	71.6(3)	N(2)–Eu(2)–O(9)	78.3(3)	N(2)–Eu(2)–O(10)	139.2(3)
N(2)–Eu(2)–O(11)	134.5(3)	N(2)–Eu(2)–O(12)	85.2(3)	N(2)–Eu(2)–O(13)	71.1(3)
N(2)–Eu(2)–O(14)	139.2(3)	N(4)–Eu(2)–O(8)	120.9(3)	N(4)–Eu(2)–O(9)	66.4(3)
N(4)–Eu(2)–O(10)	133.6(3)	N(4)–Eu(2)–O(11)	74.1(3)	N(4)–Eu(2)–O(12)	66.1(3)
N(4)–Eu(2)–N(13)	116.7(3)	N(4)–Eu(2)–O(14)	131.0(3)	N(2)–Eu(2)–N(4)	60.6(3)

is 2.677 Å. In the case of the analogous mononuclear complex **3**, the average Eu–O and Eu–N lengths are 2.355 and 2.642 Å, respectively.[13] The crystal of **1**·2Et_2O contains moderate bimolecular π–π interactions between the phenyl rings of the dbm ligands, with an average π–π interaction distance of 3.765 Å, as shown in Figure 5. The stacking interactions are only present between the dimeric pairs.

Table 1. Selected bond lengths [Å] and angles [°] for **1**·2Et_2O.

Eu(1)–O(1)	2.335(2)	Eu(1)–O(5)	2.338(2)
Eu(1)–O(4)	2.354(2)	Eu(1)–N(2)	2.675(3)
Eu(1)–N(1)	2.679(3)	Eu(1)–O(3)	2.329(2)
Eu(1)–O(2)	2.363(2)	Eu(1)–O(6)	2.338(2)
O(1)–Eu(1)–O(2)	71.65(8)	O(1)–Eu(1)–O(3)	9.79(9)
O(1)–Eu(1)–O(4)	138.50(8)	O(1)–Eu(1)–O(5)	74.56(8)
O(1)–Eu(1)–O(6)	143.25(8)	O(2)–Eu(1)–O(3)	85.78(9)
O(2)–Eu(1)–O(4)	76.11(9)	O(2)–Eu(1)–O(5)	146.00(9)
O(2)–Eu(1)–O(6)	142.18(9)	O(3)–Eu(1)–O(4)	72.37(9)
O(3)–Eu(1)–O(5)	84.78(9)	O(3)–Eu(1)–O(6)	110.01(9)
O(4)–Eu(1)–O(5)	130.88(9)	O(4)–Eu(1)–O(6)	76.54(9)
O(5)–Eu(1)–O(6)	71.37(8)	N(1)–Eu(1)–O(1)	74.47(8)
N(1)–Eu(1)–O(2)	7.96(8)	N(1)–Eu(1)–O(3)	151.22(9)
N(1)–Eu(1)–O(4)	136.30(9)	N(1)–Eu(1)–O(5)	76.22(9)
N(1)–Eu(1)–O(6)	84.35(9)	N(2)–Eu(1)–O(1)	115.10(9)
N(2)–Eu(1)–O(2)	71.39(8)	N(2)–Eu(1)–O(3)	145.45(8)
N(2)–Eu(1)–O(4)	77.09(9)	N(2)–Eu(1)–O(5)	128.33(8)
N(2)–Eu(1)–O(6)	77.41(8)	N(1)–Eu(1)–N(2)	60.41(8)

For compound **2**, the Eu–Eu, average Eu–O, and average Eu–N distances are similar to those in **1** (6.993, 2.394, 2.687 Å, respectively), although the coordination sphere of a distorted hendecahedron (square bicapped trigonal prism; Figure 4, b)[14] for **2** is different from that for **1**. The two pyrimidine rings on the bpm ligand deviate slightly from planarity by 6.3°. The crystal of **2**·2THF exhibits two types of moderate π–π interactions, as shown in Figure 6: one is an intramolecular π–π interaction between the closer thiophene rings in a molecule and the other is a bimolecular π–π interaction between the thiophene rings of neighboring molecules. The average π–π interaction distances are 3.861 and 3.892 Å, respectively, and the stacking interactions are not extended into a one-dimensional array but are isolated between the dimeric pairs, as in **1**. We consider that these bimolecular π–π interactions, as well as the high molecular weight, might be responsible for the lack of sublimability of **1**·2Et_2O and **2**·2THF.

The dinuclear entities of **1** and **2** are considered to remain unchanged in solution. Their electrospray mass spectra (see Exp. Sect. and Figure S1 in the Supporting Information) contain peaks centered at *m/z* = 1577 and 1568 assignable to $[(dbm)_3Eu(bpm)Eu(dbm)_2]^+$ and $[(tta)_3Eu(bpm)Eu(tta)_2]^+$, respectively, thereby demonstrating the formation of dinuclear species as well as the existence of the coordinated β-diketone sensitizing (dbm or tta) and bridging (bpm) ligands in solution. Additional efforts to probe the solution structures of paramagnetic lanthanide complexes **1** and **2** by recording the ^1H NMR spectra of the diamagnetic analogues to avoid the line-broadening effect associated with paramagnetism[8] were hampered by the dissimilar reactivity of Eu^{III} and La^{III} mentioned above.

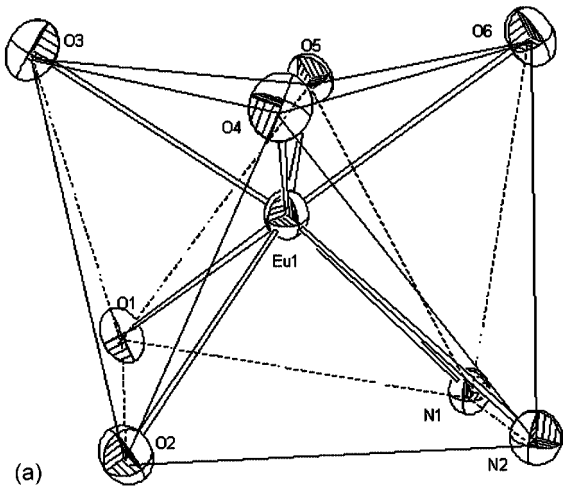

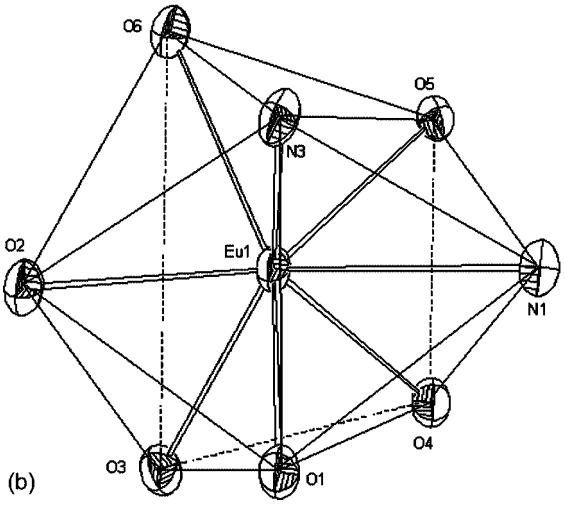

Figure 4. Coordination spheres of **1** (a) and **2** (b).

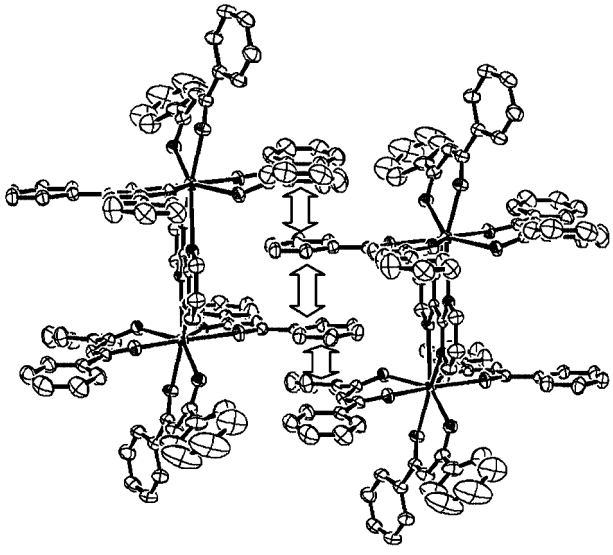

Figure 5. π-Stacked dimer in **1**·2Et_2O.

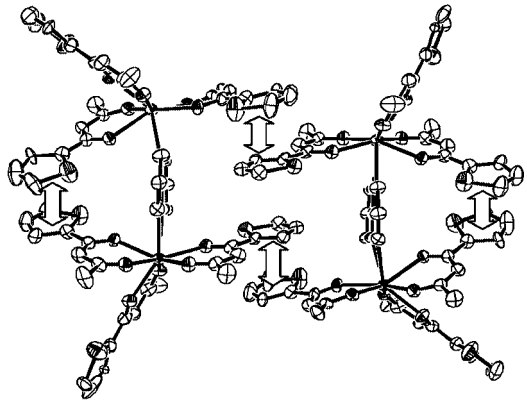

Figure 6. π-Stacked dimer in **2**·2THF.

Absorption and Photoluminescence Properties

The UV/Vis absorption spectra and the normalized PL spectra of the dinuclear europium complexes **1** and **2** and their closely corresponding mononuclear complexes **3** and **4**, in chloroform, are illustrated in Figures 7 and 8, respectively. A close inspection of Figure 7 and the spectroscopic data summarized in Table 3 reveal that the electronic excitation spectra of all the europium complexes are similar and contain features similar to those of the uncoordinated β-diketone ligands (dbmH and ttaH) regardless of the nuclearity. The strong absorption around 350 nm is attributed to the $\pi \rightarrow \pi^*$ transition of the β-diketone ligands.[15] The excitation spectra also show features similar to the absorption spectra of the Eu complexes and are red-shifted by about 30 nm (see Table 3 and Table S2 in the Supporting Information), thus indicating the indirect excitation by energy transfer from the ligand to the Eu^{III} ion.[8b,10a] Hence, we expect that the dinuclear complexes have the same luminescence mechanism mentioned in the Introduction. In fact, compounds **1**–**4** show very similar normalized PL spectra. All the complexes exhibit five peaks at 580, 591, 612, 651, and 692 nm corresponding to the $^5D_0 \rightarrow {}^7F_J$ (J = 0–4) transitions of the Eu^{3+} ion, respectively.[16] However, the full width at half maximum (FWHM) of the most intense $^5D_0 \rightarrow {}^7F_2$ transition at 612 nm in **1** and **2** is broader than that of **3** and **4**. We consider that the broadening of this hyper-

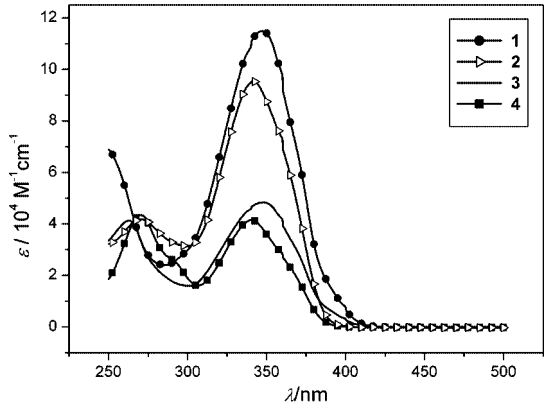

Figure 7. UV/Vis absorption spectra of **1**–**4** in chloroform solution.

sensitive transition arises from the fluxionality of the larger bimetallic complexes in solution compared to monometallic species.

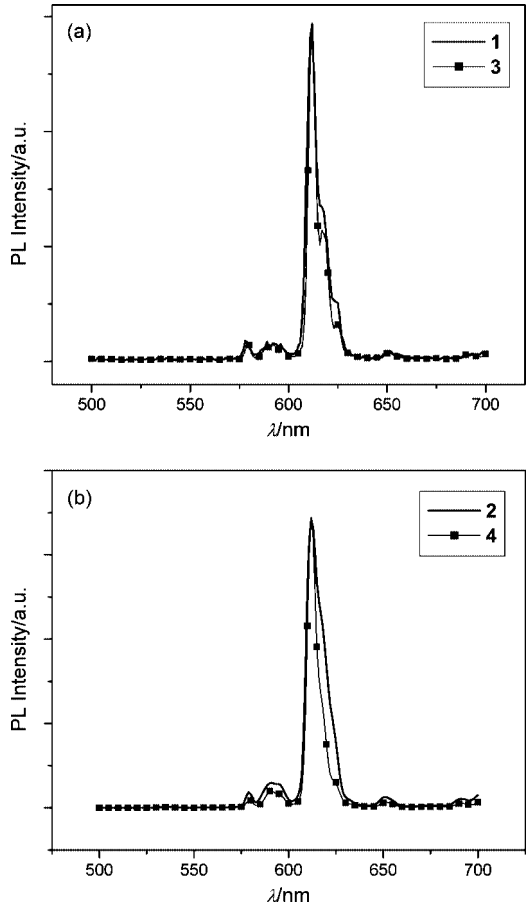

Figure 8. Normalized PL spectra of (a) dbm-containing complexes (**1**, **3**) and (b) tta-containing complexes (**2**, **4**) in chloroform solution.

The PL quantum efficiency of **1**–**4** measured in very dilute solutions of nearly the same optical density[17] decreases in the order **4** > **2** >> **1** ≈ **3** (Table 3). In addition, the europium complexes **1**, **3** containing the tta ligand show a higher efficiency than those (**2**, **4**) containing a dbm ligand due to the inductive effect of the thiophene and the fluorine substituent.[18]

The absorption and emission characteristics of **1**–**4** doped (4, 5, and 10 wt.-%) in PVK/PBD (7:3) films were also investigated. PVK, which has a good hole-transporting ability, was employed since its emission partially overlaps with the absorption spectra of the four Eu complexes. PBD is known to be a good electron-transporting and hole-blocking material and is widely used in polymer LEDs.[19] The 7:3 ratio of PVK/PBD was employed since the same mixed system has been used to fabricate white-light-emitting organic electroluminescent devices[19b] and the use of a large amount of discrete PBD would result in poor film quality. The UV/Vis spectra of the films are almost equal to that of a blank PVK/PBD host film. The minimum doping concentration at which red luminescence of Eu^{3+} appears without the occurrence of PVK/PBD host emission is 10 wt.-% for **1**–**3** and 5 wt.-% for **4**. In addition, the shape of the film PL spectrum of each compound is similar to that of the solution PL spectrum. Therefore, a 7:3 PVK/PBD mixture is a good host for these dinuclear systems.

Electroluminescent Properties

The EL devices were fabricated with a structure ITO/PEDOT (30 nm)/PVK + PBD + Eu complex (≈80 nm)/LiF (1 nm)/Al (100 nm). Chloroform and 1,2-dichloroethane (DCE) solutions were tested for spin-coating, and the DCE solution was chosen because of the better quality of its films. However, the films of tta-based complexes **2** and **4** were still of poor quality and many pin-holes and dark spots were formed immediately when the devices were operated, thus hampering the fabrication of stable EL devices with these complexes. On the other hand, dbm-containing complexes **1** and **3** show good film quality and stable red light emission. The EL spectra of **1**- and **3**-based devices (in Figure 9) resemble their PL spectra, thus the emission originates from Eu^{3+} and differs only in the intensity at 593 and 625 nm. Nonetheless, **1** emits pure red light with the CIE color coordinate (0.66, 0.34) while **3** emits red-orange light with the CIE color coordinate (0.65, 0.33). The CIE color coordinate of NTSC pure red is (0.67, 0.33). Generally, in the blended system the CIE color coordinate is known to vary as the current density increases[6,20] but the extent of such a change in **1** is much smaller than in **3**, as shown in Figure 10. The EL device with **1** has a turn-on voltage (V_T) of 12 V, a maximum brightness (L_{max}) of 25.4 cd m^{-2} at 16 V (Figure 11), and a quantum efficiency (η_{EL}) of 0.021% at 11 V. The EL characteristics of the **3**-

Table 3. Spectroscopic properties in $CHCl_3$ solution.

Complex	λ_{abs} [nm] (ε [10^4 M^{-1} cm^{-1}])	λ_{ex} [nm]	λ_{em} [nm] (η)[a]	FWHM [nm]
1	347 (11.5), 250 (6.9)	388	612 (0.0016)	7
2	341 (9.5), 271 (4.2)	379, 289, 254	612 (0.0624)	11
3	348 (4.8), 263 (4.1)	388, 286(w)[b]	612 (0.0029)	5
4	340 (4.2), 270 (4.3)	373, 312, 289, 252	612 (0.105)	6
dbmH	346, 257	–	–	–
ttaH	350, 264	–	–	–
bpm	250	–	–	–
phen	265	–	–	–

[a] PL quantum efficiency was determined in CH_2Cl_2 solution by using quinine sulfate dihydrate in 1 N H_2SO_4 solution (η = 0.55) as a standard.[16] [b] w: weak.

based device are similar to those of the **1**-based device, with V_T = 12 V, L_{max} = 30.2 cd m^{-2} at 14 V, and η_{EL} = 0.012 at 11 V (see Figure S3 in the Supporting Information).

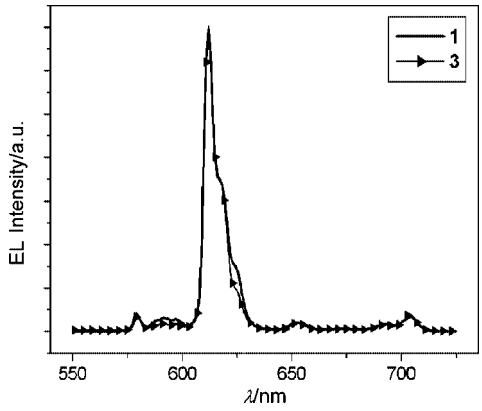

Figure 9. Comparison with normalized EL spectra of **1**- and **3**-based devices.

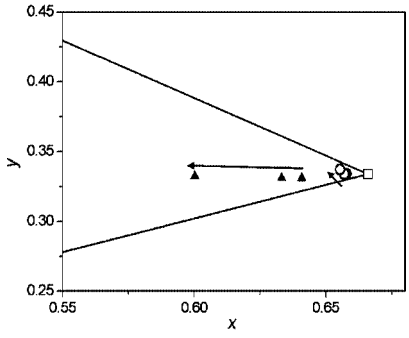

Figure 10. CIE color coordinates of **1**- (○) and **3**-based devices (▲) at a current density of 10, 20, and 100 mA cm^{-2} and the NTSC pure red (□).

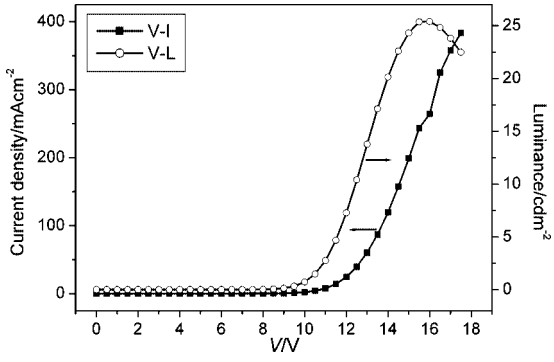

Figure 11. I-V-L characteristics of the **1**-based device.

Conclusions

Two new dinuclear Eu^{III} complexes with formula $[Eu_2L_6(bpm)]$ have been synthesized and fully characterized. Single-crystal X-ray diffraction analyses reveal their dimeric structures formed due to intermolecular π–π interactions, which seem to contribute to the lack of sublimability to some degree. It seems that the solution PL efficiency depends more on the β-diketone sensitizing ligand than the nuclearity or the bridging ligand. The dinuclear compounds are also considered to follow the luminescence mechanism adopted in mononuclear lanthanide complexes. $[Eu_2(dbm)_6(bpm)]$ (**1**) readily forms a polymer EL device ITO/PEDOT (30 nm)/PVK + PBD + Eu complex (≈80 nm)/LiF (1 nm)/Al (100 nm) that produces pure red EL. Overall, the dinuclear system shows similar thermal stability, improved EL color purity, and comparable EL efficiency with respect to the corresponding mononuclear system. Nonetheless, in order to further confirm the concept of dinuclear europium systems in developing pure red EL materials, a synthetic route to sublimable dinuclear europium complexes needs to be developed. A search for ligand systems that can not only block the formation of intermolecular π–π interactions but also have good carrier-transporting ability is in progress.

Experimental Section

Materials: The experiments were carried out using standard Schlenk techniques. THF and *n*-hexane were distilled from Na-K alloy, diethyl ether (Et_2O) from Na-benzophenone ketyl, and CH_2Cl_2 from CaH_2. Ethanol and other reagents were used without any further purification after purchase from Hayman (ethanol), Aldrich (dbmH, ttaH, phen, $EuCl_3·6H_2O$), and Lancaster (bpm). $[Eu(dbm)_3(phen)]$ (**3**) and $[Eu(tta)_3(phen)]$ (**4**) were prepared according to a literature procedure,[12b] purified from THF/*n*-hexane and dried at 110 °C at 10^{-5} Torr for 6 h. Chemicals for EL devices were purchased from Aldrich [poly(9-vinylcarbazole) (PVK), 2-(4-biphenylyl)-5-(4-*tert*-butylphenyl)-1,3,4-oxadiazole (PBD), LiF, Al, and anhydrous 1,2-dichloroethane (DCE)] and Bayer [poly(styrenesulfonate)-doped poly(3,4-ethylenedioxythiophene) (PEDOT)] and used without further purification.

Synthesis of $[Eu_2(dbm)_6(bpm)]$ (1): Aqueous NaOH solution (3.0 mL, 1.0 M) and then, rapidly, an aqueous solution of $EuCl_3·6H_2O$ (0.37 g, 1.0 mmol) were added to a 30-mL ethanol solution of dbmH (0.67 g, 3.0 mmol) and bpm (0.079 g, 0.50 mmol) in a two-necked flask. The reaction mixture was refluxed at 60 °C for 12 h and cooled to ambient temperature to give a yellow precipitate, which was filtered off and washed with water and ethanol. The resulting solid was air-dried and recrystallized from a CH_2Cl_2/Et_2O solution as yellow crystals of **1**·2Et_2O. The solvate Et_2O molecules in the crystals were removed at 110 °C under a vacuum of 10^{-5} Torr for 6 h after grinding. Yield: 1.1 g (59%). M.p. 240–242 °C. T_{d5} = 300 °C. IR (KBr): $\tilde{\nu}$ = 444, 511, 609, 656, 670, 687, 719, 940, 1070, 1218, 1310, 1408, 1458, 1478, 1522, 1547, 1595 cm^{-1}. $C_{98}H_{72}Eu_2N_4O_{12}$ (1802.4): calcd. C 65.33, H 4.03, N 3.11; found C 64.88, H 4.02, N 3.12. MS (ESI): *m*/*z* = 159 [bpm + H]$^+$, 225 [dbmH + H]$^+$, 756 $[(dbm)_2Eu(bpm)]^+$, 822 $[(dbm)_3Eu + H]^+$, 914 $[(dbm)_2Eu(bpm)_2]^+$, 980 $[(dbm)_3Eu(bpm) + H]^+$, 1048 $[(dbm)_4Eu + 2H]^+$, 1577 $[(dbm)_3Eu(bpm)Eu(dbm)_2]^+$.

Synthesis of $[Eu_2(tta)_6(bpm)]$ (2): This complex was synthesized by an analogous method to **1** but with 3.0 mmol (0.67 g) of ttaH. Recrystallization from THF/*n*-hexane afforded light-yellow crystals of **2**·2THF. The solvate THF molecules in the crystals were removed at 110 °C under a vacuum of 10^{-5} Torr for 6 h after grinding. Yield: 1.1 g (59%). M.p. 268–270 °C. T_{d5} = 305 °C. IR (KBr): $\tilde{\nu}$ = 499, 582, 641, 683, 759, 793, 935, 1061, 1143, 1187, 1231, 1251, 1308, 1354, 1413, 1459, 1509, 1540, 1580, 1600 cm^{-1}.

Table 4. Crystallographic data for **1**·2Et_2O and **2**·2THF.

	1·2Et_2O	**2**·2THF
Formula	$C_{49}H_{36}EuN_2O_6$·($C_4H_{10}O$)	$C_{56}H_{30}Eu_2F_{18}N_4O_{12}S_6$·($C_8H_{16}O_2$)
M	974.88	1933.33
Crystal system	monoclinic	triclinic
Space group	$P2_{1/n}$	$P\bar{1}$
a [Å]	10.9094(13)	10.198(2)
b [Å]	23.016(3)	18.211(4)
c [Å]	19.176(2)	23.169(5)
α [°]	90	102.378(4)
β [°]	99.202(2)	102.121(4)
γ [°]	90	100.233(4)
V [Å^3]	4752.9(10)	3995.7(15)
Z	4	2
D_{calc} [g cm^{-3}]	1.362	1.607
μ [mm^{-1}]	1.372	1.813
No. of reflections measured	55647	46354
No. of reflections used (R_{int})	11275 (0.0518)	18300 (0.0851)
Final R [$I > 2\sigma(I)$] R_1,[a] wR_2[b]	0.0337, 0.0690	0.0763, 0.2085
Goodness of fit on F^2	0.930	0.960

[a] $R_1 = \Sigma||F_0| - |F_c||/\Sigma|F_0|$. [b] $wR_2 = [\Sigma\{w(F_0^2 - F_c^2)^2\}/\Sigma\{w(F_0^2)\}^2]^{1/2}$, where $w = 1/[\sigma^2(F_0^2) + (xP)^2 + yP]$ and $P = (F_0^2 + 2F_c^2)/3$.

$C_{56}H_{30}Eu_2F_{18}N_4O_{12}S_6$ (1789.8): calcd. C 37.59, H 1.69, N 3.13; found C 37.72, H 1.58, N 3.21. MS (ESI): m/z = 159 [bpm + H]$^+$, 181 [bpm + Na]$^+$, 752 [$(tta)_2Eu(bpm)$]$^+$, 910 [$(tta)_2Eu(bpm)_2$]$^+$, 1522 [$(tta)_2Eu(bpm)_2Eu(tta)_2$ + OH$^-$]$^+$, 1568 [$(tta)_3Eu(bpm)$-$Eu(tta)_2$]$^+$.

X-ray Crystallography: Suitable crystals of **1**·2Et_2O and **2**·2THF were obtained by diffusion of Et_2O into a CH_2Cl_2 solution and *n*-hexane into a THF solution, respectively. Reflection data were collected on a Bruker 1 K SMART CCD-based diffractometer with graphite-monochromated Mo-K_α radiation (λ = 0.71073 Å) at 293 K. A hemisphere of reflection data was collected as ω scan frames with a width of 0.3° per frame and an exposure time of 10 s per frame. Cell parameters were determined and refined with the SMART program.[21] Data reductions were performed with SAINT,[22] which corrects for Lorentz polarization effects; no corrections for crystal decay were required. Empirical absorption corrections were applied with SADABS.[23] The structures of the compounds were solved by direct methods and refined by full-matrix least-squares methods using the SHELXTL program package with anisotropic thermal parameters for all non-hydrogen atoms. Hydrogen atoms were placed at their geometrically calculated positions and refined riding on the corresponding carbon atoms with isotropic thermal parameters. Crystal data for both systems are summarized in Table 4.

CCDC-250346 (for **1**) and -250347 (for **2**) contain the supplementary crystallographic data for this paper. These data can be obtained free of charge from The Cambridge Crystallographic Data Center via www.ccdc.cam.ac.uk/data_request/cif.

Instrumentation: Infrared spectra were obtained from KBr pellets with a Bruker EQUINOX-55 spectrometer. Elemental analyses were performed on an EA1110-FISONS (CE Instruments) by the Environmental Analysis Laboratory at KAIST. Electrospray mass spectra were measured on a Mariner instrument at the Korea Basic Science Institute. Melting points were determined on an Electrothermal IA 9100 apparatus. Thermogravimetric analyses (TGA) were carried out under a nitrogen atmosphere at a heating rate of 10 °C min^{-1} with a Dupont 9900 Analyzer. UV/Vis spectra were obtained with a Jasco V-530 spectrophotometer. PL spectra and PL quantum efficiency were recorded with a Spex Fluorog-3 luminescence spectrometer. Excitation spectra were obtained with a Perkin–Elmer LS 50B luminescence spectrometer.

Fabrication of EL Devices: The configuration of the EL device was ITO/PEDOT/emitting layer (EML)/LiF/Al. PEDOT, used as a hole-injection layer, was spin-coated onto a pre-cleaned ITO/glass substrate at a spin speed of 1500 rpm for 60 s. Then, a layer of Eu complex-doped PVK/PBD (7:3) was fabricated by spin-coating from their 1,2-dichloroethane solutions (10–11 mg mL^{-1}) at 1250 rpm for 60 s. The film thickness of the EML was determined with a TENCOR alpha-step 500 profiler and was approximately 80 nm. LiF (1 nm) and Al (100 nm) were deposited on top of the EML using the vacuum-evaporation method at a pressure of 10^{-6} Torr. EL spectra were obtained with a Minolta CS-1000. The current–voltage and luminance–voltage characteristics were recorded with a current–voltage source (Keithley 238) and a luminescence detector (Minolta LS-100), respectively. All EL measurements were carried out at room temperature under an ambient atmosphere.

Acknowledgments

The authors gratefully acknowledge financial support from the Korea Science and Engineering Foundation (R02-2002-000-00057-0), CMDS, MOCIE, and the BK 21 Project.

[1] a) S. Miyata, H. S. Nalwa, *Organic Electroluminescent Materials and Devices*, Gordon and Breach Publishers, The Netherlands, **1997**; b) D. M. Roundhill, J. P. Fackler, *Optoelectronic Properties of Inorganic Compounds*, Plenum Press, New York, **1999**; c) U. Mitschke, P. Bauerle, *J. Mater. Chem.* **2000**, *10*, 1471; d) L. S. Hung, C. H. Chen, *Mater. Sci. Eng., R* **2002**, *39*, 143.

[2] a) E. Cariati, J. Bourassa, P. C. Ford, *Chem. Commun.* **1998**, 1623; b) M. Montalti, L. Prodi, N. Zaccheroni, L. Charbonniere, L. Douce, R. Ziessel, *J. Am. Chem. Soc.* **2001**, *123*, 12694; c) V. W.-W. Yam, S.-K. Yip, L.-H. Yuan, K.-L. Cheung, N. Zhu, K.-K. Cheung, *Organometallics* **2003**, *22*, 2630; d) K. K.-W. Lo, C.-K. Chung, T. K.-W. Lee, L.-H. Lui, K. H.-K. Tsang, N. Zhu, *Inorg. Chem.* **2003**, *42*, 6886.

[3] a) L. Fabbrizzi, F. Foti, M. Licchelli, P. M. Maccarini, D. Sacchi, M. Zema, *Chem. Eur. J.* **2002**, *8*, 4965; b) M. Hissler, J. E. McGarrah, W. B. Connick, D. B. Geiger, S. D. Cummings, R. Eisenberg, *Coord. Chem. Rev.* **2000**, *208*, 115.

[4] a) Y. Hamada, *IEEE Trans. Elec. Dev.* **1997**, *44*, 1208; b) C. H. Chen, J. Shi, *Coord. Chem. Rev.* **1998**, *171*, 161; c) S. Wang,

Coord. Chem. Rev. **2001**, *215*, 79; d) C. W. Tang, S. A. VanSlyke, *Appl. Phys. Lett.* **1987**, *51*, 913; e) S. Lamansky, P. Djurovich, D. Murphy, F. Abdel-Razzaq, H.-E. Lee, C. Adachi, P. E. Burrows, S. R. Forrest, M. E. Thompson, *J. Am. Chem. Soc.* **2001**, *123*, 4304.

[5] a) J. Kido, Y. Okamoto, *Chem. Rev.* **2002**, *102*, 2357 and references cited therein; b) M. D. McGehee, T. Bergstedt, C. Zhang, A. P. Saab, M. B. O'Regem, G. C. Bazan, V. I. Srdanov, A. J. Heeger, *Adv. Mater.* **1999**, *11*, 1349; c) G. Yu, Y. Liu, X. Wu, D. Zhu, H. Li, L. Jin, M. Wang, *Chem. Mater.* **2000**, *12*, 2537; d) X. Jiang, A. K.-Y. Jen, D. Huang, G. D. Phelan, T. M. Londergan, L. R. Dalton, *Synth. Met.* **2002**, *125*, 331; e) M. Sun, H. Xin, K.-Z. Wang, Y.-A. Zhang, L.-P. Jin, C.-H. Huang, *Chem. Commun.* **2003**, 702; f) F. Liang, Q. Zhou, Y. Cheng, L. Wang, D. Ma, X. Jing, F. Wang, *Chem. Mater.* **2003**, *15*, 1935; g) P.-P. Sun, J.-P. Duan, H.-T. Shih, C.-H. Cheng, *Appl. Phys. Lett.* **2002**, *81*, 792.

[6] a) Y. Wang, D. Song, C. Seward, Y. Tao, S. Wang, *Inorg. Chem.* **2002**, *41*, 5187.

[7] W.-Y. Yang, L. Chen, S. Wang, *Inorg. Chem.* **2001**, *40*, 507.

[8] a) M. M. Castaño-Briones, A. P. Bassett, L. L. Meason, P. R. Ashton, Z. Pikramenou, *Chem. Commun.* **2004**, 2832; b) A. P. Bassett, S. W. Magennis, P. B. Glover, D. J. Lewis, N. Spencer, S. Parsons, R. M. Williams, L. De Cola, Z. Pikramenou, *J. Am. Chem. Soc.* **2004**, *126*, 9413.

[9] J.-C. G. Bünzli, F. Besançon, *Phys. Chem. Chem. Phys.* **2005**, *7*, 2191.

[10] a) V. Patroniak, P. N. W. Baxter, J.-M. Lehn, Z. Hnatejko, M. Kubicki, *Eur. J. Inorg. Chem.* **2004**, 2379; b) K. Zeckert, J. Hamacek, J.-P. Rivera, S. Floquet, A. Pinto, M. Borkovec, C. Piquet, *J. Am. Chem. Soc.* **2004**, *126*, 11589.

[11] D. Zhao, W. Li, Z. Hong, X. Liu, C. Liang, D. Zhao, *J. Lumin.* **1999**, *82*, 105.

[12] a) J. Kido, H. Hayase, K. Hongawa, K. Nagai, K. Okuyama, *Appl. Phys. Lett.* **1994**, *65*, 2124; b) T. Sano, M. Fujita, T. Fujii, Y. Hamada, K. Shibata, K. Kuroki, *Jpn. J. Appl. Phys.* **1995**, *34*, 1883.

[13] a) M. O. Ahmed, J.-L. Liao, X. Chen, S.-A. Chen, J. H. Kaldis, *Acta Crystallogr., Sect. E* **2003**, *59*, m29; b) Y. Jian, H. Xian, Z. Zhong-Yuan, L. Li, *J. Struct. Chem.* **1989**, *8*, 187.

[14] a) C. W. Haigh, *Polyhedron* **1996**, *15*, 605; b) S. J. Lippard, *Prog. Inorg. Chem.* **1967**, *8*, 109.

[15] a) N. J. Turro, *Modern Molecular Photochemistry*, University Science Books, Herndon, USA, **1991**, p.77; b) J.-C. G. Bünzli, E. Moret, V. Foiret, K. J. Schenk, W. Mingzhao, J. Linpei, *J. Alloys Compd.* **1994**, *207/208*, 107.

[16] L. Huang, K.-Z. Wang, C.-H. Huang, F.-Y. Li, Y.-Y. Huang, *J. Mater. Chem.* **2001**, *11*, 790.

[17] a) G. E. Hardy, W. C. Kaska, B. P. Chandra, J. I. Zink, *J. Am. Chem. Soc.* **1981**, *103*, 1074; b) H. S. Joshi, R. Jamishidi, Y. Tor, *Angew. Chem. Int. Ed.* **1999**, *38*, 2722.

[18] a) C. N. R. Rao, J. R. Ferraro, *Spectroscopy in Inorganic Chemistry*, vol. 2, Academic Press, New York, USA, **1971**; b) J. Yuan, K. Matsumoto, *Anal. Sci.* **1996**, *12*, 31.

[19] a) S. Miyata, H. S. Nalwa, *Organic Electroluminescent Materials and Devices*, Gordon and Breach Publishers, The Netherlands, **1997**, p. 203; b) J. Kido, H. Shionoya, K. Nagai, *Appl. Phys. Lett.* **1995**, *67*, 2281.

[20] a) J. Wang, R. Wang, J. Yang, Z. Zheng, M. D. Carducci, T. Cayou, N. Peyghambarian, G. E. Jabbour, *J. Am. Chem. Soc.* **2001**, *123*, 6179; b) H. Heil, J. Steiger, R. Schmechel, H. von Seggern, *J. Appl. Phys.* **2001**, *90*, 535.

[21] *SMART*, *Version 5.0, Data collection software*, Bruker AXS, Inc., Madison, WI, USA, **1998**.

[22] *SAINT*, *Version 5.0, Data integration software*, Bruker AXS, Inc., Madison, WI, USA, **1998**.

[23] G. M. Sheldrick, *SADABS*, *Program for absorption correction with the Bruker SMART system*, University of Göttingen, Germany, **1996**.

Received: May 16, 2005
Published Online: December 20, 2005

